

Detecting Selection in Low-Coverage High-Throughput Sequencing Data using Principal Component Analysis

Jonas Meisner, Anders Albrechtsen, Kristian Hanghøj

The Bioinformatics Centre, Department of Biology, University of Copenhagen, Denmark

1 Abstract

Identification of selection signatures between populations is often an important part of a population genetic study. Leveraging high-throughput DNA sequencing larger sample sizes of populations with similar ancestries has become increasingly common. This has led to the need of methods capable of identifying signals of selection in populations with a continuous cline of genetic differentiation. Individuals from continuous populations are inherently challenging to group into meaningful units which is why existing methods rely on principal components analysis for inference of the selection signals. These existing methods require called genotypes as input which is problematic for studies based on low-coverage sequencing data. Here, we present two selection statistics which we have implemented in the `PCAngsd` framework. These methods account for genotype uncertainty, opening for the opportunity to conduct selection scans in continuous populations from low and/or variable coverage sequencing data. To illustrate their use, we applied the methods to low-coverage sequencing data from human populations of East Asian and European ancestries and show that the implemented selection statistics can control the false positive rate and that they identify the same signatures of selection from low-coverage sequencing data as state-of-the-art software using high quality called genotypes. Moreover, we show that `PCAngsd` outperform selection statistics obtained from called genotypes from low-coverage sequencing data.

2 Introduction

Natural selection is the main driver of local adaptation. Instead of tracing the adaptive phenotypic trait, a “reverse ecology” approach is commonly applied [12], where the genetic variant encoding for a beneficial trait is first identified followed by the underlying mechanism of the adaptive phenotype. This enables mapping of the genetic architecture of phenotypic adaptability driven by natural selection ([6] for review on human populations). A common approach to identify candidates under selection is based on outliers in an empirical distribution of differentiation between two or more groups of predefined populations. In its simplest form, it finds the variants with the biggest difference in allele frequency between two predefined populations. One of many methods based on this notion is Population Branch Statistics [30], an estimator of genetic differentiation based on allelic changes estimated with the fixation index (F_{ST}). It identifies candidate regions as strong deviations from an empirical distribution between a target population, a closely related sister population and an

outgroup. However, homogeneous discrete groupings of the populations is required for many of these models, albeit exceptions exist [2].

The reduced expenses for whole genome DNA sequencing, thanks to advanced High-throughput DNA sequencing technologies, has facilitated larger sample sizes in population genetics studies in the recent years, including samples with similar genetic ancestry [4, 13, 29, 25, 19, 28]. Identifying signatures of selection in populations of similar genetic ancestry can result in arbitrary population assignments when using methodologies that require discrete groups of populations. This can lead to reduced power and increased false positive rates as allele frequencies are estimated from non-homogeneous populations. Instead of coercing samples into groups, an alternative approach is to account for the continuous cline of genetic differentiation in the selection analysis. Recent studies have shown that principal components analysis (PCA) of genetic data can detect signals of selection in continuous populations [14, 7]. Briefly, the idea is to use PCA to infer a weight for each variant which is scaled to reflect genetic drift. Variants with deviating statistics from the null distribution of what is expected under pure drift are candidates for selection. This approach has been applied to several datasets, including populations of humans [13, 7, 3], wheat [22], cod [26], turbot [18], and tiger mosquito [9].

Two commonly used software that accounts for continuous population differentiation when performing selection scans are `FastPCA` [7] and `pcadapt` [14, 23]. Both software use called genotypes as input to obtain the top K principal components (PCs) and variant weights through a truncated singular value decomposition (SVD) [10, 24]. However, they differ in their derived test statistics. `pcadapt` uses robust Mahalanobis distance [15] to evaluate all top K PCs for estimating z -scores, whereas `FastPCA` tests normalized variant weights for each PC separately. Both test statistics follow χ^2 distributions from which a p -value for each polymorphic site is obtained.

In this study, we extended the `FastPCA` [7] and `pcadapt` [14] selection statistics to account for genotype uncertainty by leveraging the PCs and variant weights estimated iteratively in the `PCAngsd` framework [17] using genotype likelihoods. This allows us to analyze low-coverage data and naturally impute missing data based on individual allele frequencies estimated from the top K inferred PCs. We apply the novel methods to populations of East Asian ancestry and European ancestry using the low-coverage data of the 1000 Genome Project [4] and demonstrate that we can identify known signatures of selection within these two ancestries. The candidates under selection were verified using the corresponding high quality genotype data from the 1000 Genome Project. The test statistics are implemented in the `PCAngsd` framework [17] that is available at <https://github.com/rosemeis/pcangsd>.

3 Materials and Methods

We assume that variable sites are diallelic and the major and minor allele are known such that genotypes are expected to follow a Binomial model. In low-coverage sequencing data, genotypes are unobserved and genotype likelihoods are therefore used instead to account for the uncertainty in sequencing process. We use the iterative procedure in `PCAngsd` [17] to estimate individual allele frequencies that can be seen as the underlying parameters in the Binomial sampling processes of the genotypes accounting for population structure. In the following, we will denote N as the number of individuals and M as the number of sites. We can then define the posterior genotype dosage as follows for individual i in site j

$$\mathbb{E}[G_{ij} | X_{ij}, \hat{\pi}_{ij}] = \sum_{g=0}^2 g P(G_{ij} = g | X_{ij}, \hat{\pi}_{ij}), \quad (1)$$

for $i = 1, \dots, N$ and $j = 1, \dots, M$, where $P(G_{ij} = g | X_{ij}, \hat{\pi}_{ij})$ is the posterior genotype probability of genotype g with X being the observed sequencing data, and $\hat{\pi}$ being the individual allele frequency. Details of deriving the posterior genotype from genotype likelihoods can be found in the supplementary material (Equation S1-S2). Missing data is imputed based on population structure based on the posterior genotype dosages. We standardize the dosage under the assumption of a Binomial model,

$$y_{ij} = \frac{\mathbb{E}[G_{ij} | X_{ij}, \hat{\pi}_{ij}] - 2\hat{f}_j}{\sqrt{2\hat{f}_j(1 - \hat{f}_j)}}. \quad (2)$$

Here \hat{f} is the estimated allele frequency at site j based on all of the samples. We then perform truncated SVD [10] on the full standardized data matrix ($N \times M$) to extract the top K principal components (PCs) that capture population structure in the dataset

$$\hat{\mathbf{Y}} = \mathbf{U}_{[1:K]} \mathbf{S}_{[1:K]} \mathbf{V}_{[1:K]}^T, \quad (3)$$

where $\mathbf{U}_{[1:K]}$ represents the captured population structure of the individuals and $\mathbf{V}_{[1:K]}$ represents the scaled variant weights, while $\mathbf{S}_{[1:K]}$ is the diagonal matrix of singular values. This low-rank approximation along with the standardized matrix \mathbf{Y} are all we need to estimate the two test statistics for low-coverage sequencing data.

3.1 FastPCA statistic

The selection statistic derived in Galinsky et al. (2016) [7], hereafter referred to as **FastPCA**, tries to detect selection by looking for variants that significantly differentiate from genetic drift along an axis of genetic variation. They define the selection statistics for the k -th principal component to be the properly normalized variant weights, using the properties of an eigenvector, such that they are standard normal distributed. The selection statistics are then defined as follows in our setting for genotype likelihood data

$$d_{jk} = v_{jk} \sqrt{M}, \quad (4)$$

$$d_{jk} \sim \mathcal{N}(0, 1), \quad (5)$$

$$d_{jk}^2 \sim \chi_1^2, \quad (6)$$

for $j = 1, \dots, M$ and $k = 1, \dots, K$. v_{jk} is the variant weight for the k th component at site j . The squared statistic will then follow a χ^2 -distribution with 1 degree of freedom. This statistic is implemented in the **PCAngsd** framework and referred to as **PCAngsd-S1**.

3.2 pcadapt statistic

The test statistic implemented in **pcadapt** [14] is based on a robust Mahalanobis distance of the standardized estimates in a multiple linear regression for each site. The regression model is defined as follows in our setting for genotype likelihood data

$$\mathbf{y}_j = \mathbf{U}_{[1:K]}\boldsymbol{\beta}_j + \boldsymbol{\epsilon}_j, \quad (7)$$

for $j = 1, \dots, M$, with $\boldsymbol{\beta}_j$ being the regression coefficients, and $\boldsymbol{\epsilon}_j$, the residual vector for site j . The coefficients are easily derived using the normal equation and properties of the previously computed truncated SVD (Equation 3), thus $\boldsymbol{\beta}_j = \mathbf{S}_{[1:K]}\mathbf{V}_{[j,1:K]}$. A z -score of the regression coefficients in site j are defined as

$$\mathbf{z}_j = \boldsymbol{\beta}_j / \sqrt{\frac{(\mathbf{y}_j - \hat{\mathbf{y}}_j)^T(\mathbf{y}_j - \hat{\mathbf{y}}_j)}{N - K}}, \quad (8)$$

with $\hat{\mathbf{y}}_j$ being the vector of low-rank approximations in site j (Equation 3). The test statistic is computed as a robust Mahalanobis distance of \mathbf{z}_j , where the squared distance will be χ_K^2 distributed as described in Luu et al. (2016) [14]. We use standardized expected genotypes y_{ij} (Equation 2) for genotype likelihood data, hereafter referred to as **PCAngsd-S2**, instead of using known genotypes as **pcadapt**. Note, that we correct for inflation using the genomic inflation factor [5], inline with the recommendations [14], in all analysis based on the **pcadapt** or **PCAngsd-S2** statistics. See QQ-plot in Figure S1 and S2 for examples of the uncorrected **PCAngsd-S2** test statistic.

3.3 1000 Genomes Project data

We applied the two selection statistics implemented in the **PCAngsd** framework to the low-coverage data of the 1000 Genomes Project (phase 3). Specifically, we tested two sets of populations, one with East Asian ancestry with 400 unrelated individuals from four East Asian populations (CHB, CHS, CDX, and KHV), and one with European ancestry with 404 unrelated individuals from four European populations (CEU, GRB, IBS, and TSI). High quality genotype data is available for all the individuals analyzed. First, we calculated genotype likelihoods (GL) from the low-coverage data using **ANGSD** [8], restricting to polymorphic sites with a minor allele frequency of 5% in the high quality genotype data for each set of populations. In total 5.8 and 6 million polymorphic sites are retained in the Asian and European population sets, respectively. We used the GL data as input to **PCAngsd** to compute the two selection statistics (**PCAngsd-S1**, **PCAngsd-S2**) for the population sets. To verify the results obtained from the low-coverage data, we also analyzed the same variable sites from the high quality genotype (HQQ) data using **PCAngsd**, **pcadapt** (default settings), and **FastPCA** (**fastmode: YES**, following [7]).

To compare the performance of **pcadapt** and **FastPCA** on low-coverage data, we called genotypes for the same variants described above from the low-coverage data using **bcftools** [11] and generated two data sets, one excluding all genotype calls with genotype quality < 20 (**CG standard**) and one including all called genotypes (**CG***).

4 Results and Discussion

To test the performance of the two selection statistics (**PCAngsd-S1** and **PCAngsd-S2**), implemented in **PCAngsd**, on continuous genetic differentiation in low-coverage data sets, we used data from the 1000 Genomes Project [4]. We tested four populations with East Asian ancestry and four populations with European ancestry and identified known signatures of selection in both ancestries. We compared the results to **FastPCA** and **pcadapt** applied to HQG data and two data sets based on

called genotypes from the low-coverage data, **CG standard** where all genotype calls with a genotype quality lower than 20 were excluded and **CG*** containing all called genotypes.

We applied the selection statistics to 400 individuals from four populations (CHB, CHS, KHV, CDX) with East Asian ancestry. First, we performed PCA on the GL data using **PCAngsd** [17] where we observed a continuous separation between the northern (CHB, CHS) and southern (KHV, CDX) populations on the first principal component (PC) (Figure 1). **FastPCA** and **pcadapt** obtained a similar pattern on the HQG data (Figure 1). PC2 obtained from **PCAngsd** and **pcadapt** separate the Vietnamese Kinh population (KHV) and Chinese Dai population (CDX) (Figure 1). When applied to the **CG standard** data, **FastPCA** and **pcadapt** could not recover the continuous separation on PC1. Instead we observe within population variance driven by the bias from genotype calling on low depth data when genotype quality filters are applied [20]. Therefore, **CG standard** data was not used for downstream selection scan comparisons. The PCA obtained from genotype data without quality filter **CG*** did not show the same problems and recovered the continuous separation on PC1 and was included in the following selection scan analyses 1.

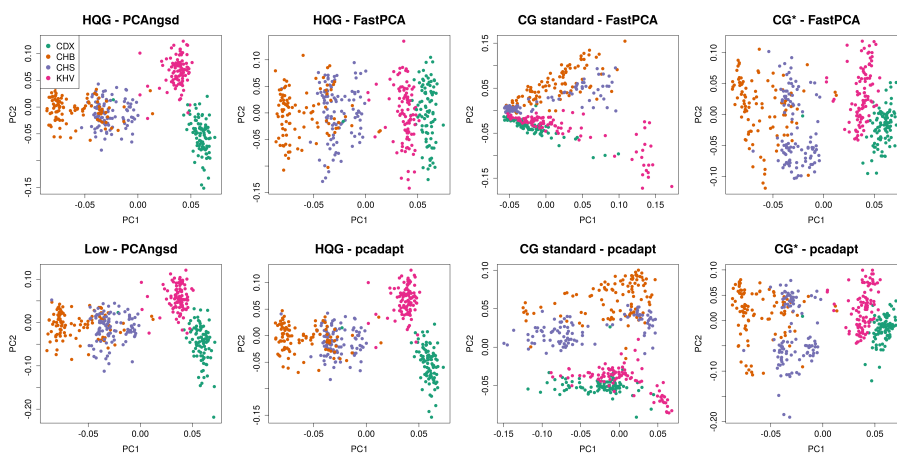


Figure 1: PC1 against PC2 of four East Asian populations obtained from **PCAngsd**, **FastPCA** and **pcadapt**. **HQG**: High quality genotype data, **Low**: Low-coverage data, **CG standard**: Called genotypes from low-coverage data with genotype quality threshold on 20, **CG***: Called genotypes from low-coverage data.

We applied the test statistics on the variant weights inferred along the two PCs and scan for genomic regions with significant differentiation on the continuous north-to-south cline on PC1 and separation of KHV and CDX on PC2. We identify several candidates under selection along PC1 (Figure 2). After multiple testing correction using Bonferroni (p -value $< 9 \times 10^{-9}$, $\alpha = 0.05$), we find significant signals of differentiation in variants overlapping *FADS2* (chr11), *IGH* cluster (chr14), *ABCC11* (chr16), and *LILRA3* (chr19). These signatures of selection have been described in previous studies of selection on continuous differentiation in Han Chinese populations [13, 3]. Interestingly, **PCAngsd** also identifies a genomic region overlapping *CR1* on the low coverage data, previously described by Chiang and colleagues [3] and the NIPT data [13]. We find a similar signal using the other software on the HQG although not significant. **FastPCA** and **pcadapt** find the same candidates with significant differentiation when applied to the HQG data.

Both **PCAngsd** and **pcadapt** identify population structure on PC2 separating CDX and KHV

and find the same two significant candidate regions: *HLA-cluster* (chr6) (also observed in [3]) and *Olfactory cluster* (chr11) (Figure 2). The variants overlapping the Olfactory cluster show strong LD pattern on both sides of the centromere, a challenging region to assemble potentially resulting in systematic biases, however, we do note that the pattern is present both on the HQG and low-coverage data (Figure 2 and S1). *PCAngsd-S2* and *pcadapt* identify a single significant variant on chr3 and chr9 in the HQG data. Following a test for Hardy-Weinberg equilibrium (HWE) accounting for population structure [16], we find that these two variants are the only top hits among selection candidates that significantly deviate from HWE (Table S1). This indicates genotype calling related biases as the variants are not candidates under selection in the low-coverage sequencing data.

When *FastPCA* and *pcadapt* are applied to the low depth data, *CG**, not all of these signals are identified despite PC1 separating the four populations. We observed highly inflated statistics with significant false positive signals present genome-wide blurring the signals observed on the HQG data (Figure 2).

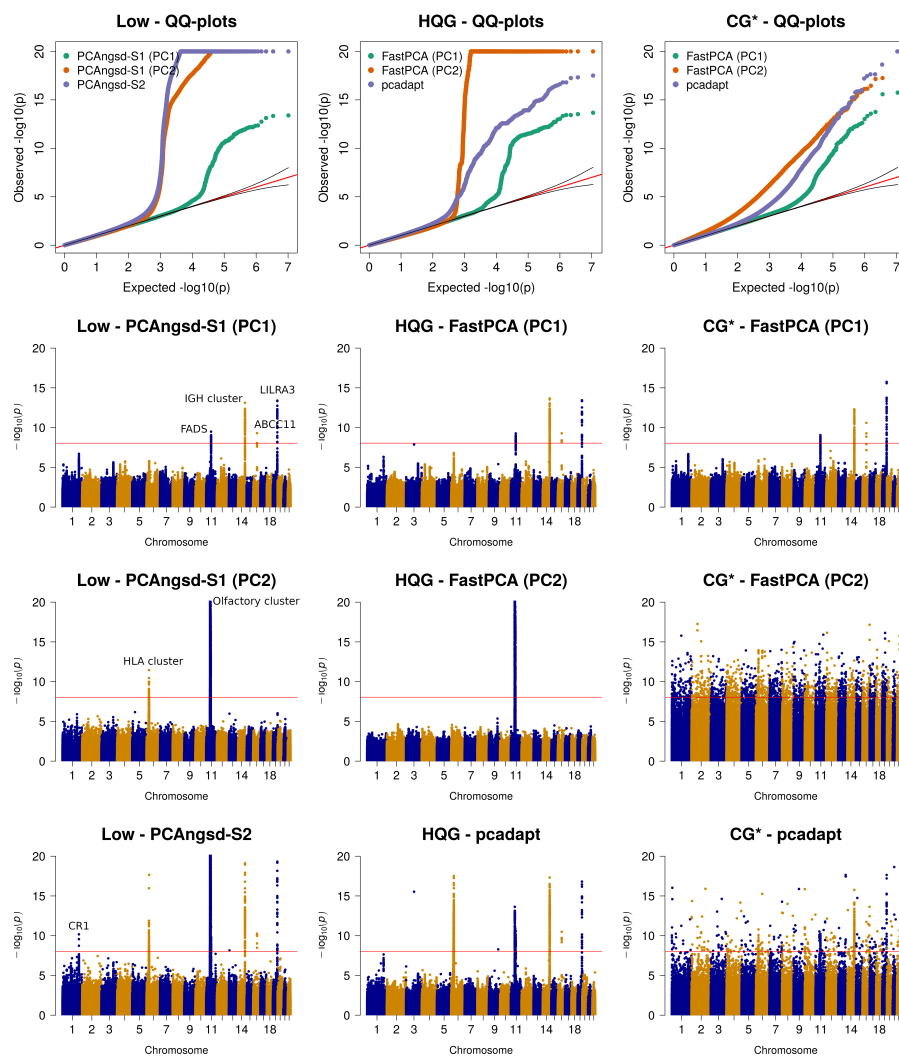


Figure 2: Selection scan of East Asian populations. QQ and Manhattan plots of the selection statistics from PCAngsd, FastPCA and pcadapt applied to the four East Asian populations obtained. Red horizontal line is the Bonferroni adjusted significance level. PCAngsd-S2 and pcadapt has been corrected for genomic inflation. HQG: High quality genotype data, Low: Low-coverage data, CG*: Called genotypes from low-coverage data.

Similarly to the populations with East Asian ancestry, we also performed selection scans of 404 individuals from four populations (CEU, GBR, IBS, TSI) with European ancestry. We know from previous research that lactase persistence and skin and hair pigmentation distributions show a north-south cline within European populations [1, 21, 27], where the northern European populations have higher lactase persistence and lighter pigmentation than the southern European populations. We first performed PCA on the GL data using PCAngsd [17] (Figure 3) where we observed a

continuous separation between the northern (CEU, GBR) and southern (TSI, IBS) populations on the first PC. `FastPCA` and `pcadapt` obtained a similar pattern on the HQG data (Figure 3). As for the East Asian scenario, `FastPCA` and `pcadapt` could not recover the continuous separation on PC1 on the CG standard data which was excluded from further analysis. The PCA obtained from CG* data set recovered the continuous separation on PC1 and was used in the following selection scan analyses 3.

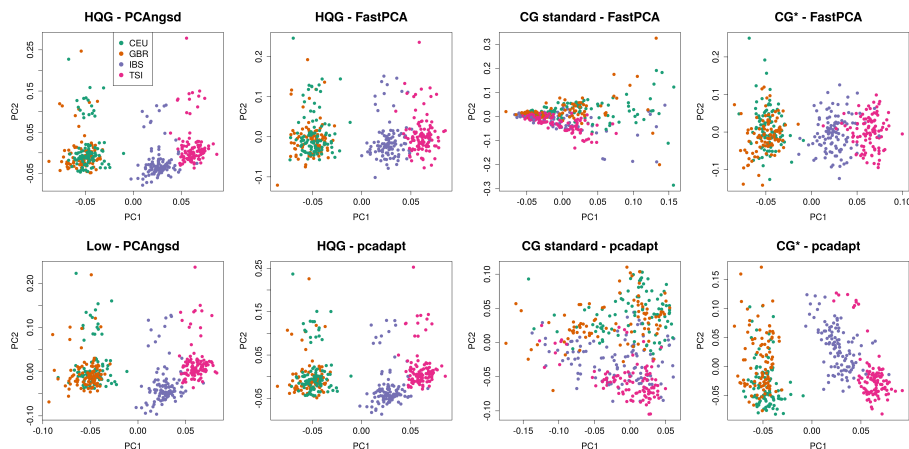


Figure 3: PC1 against PC2 of four European populations obtained from `PCAngsd`, `FastPCA` and `pcadapt`. HQG: High quality genotype data, Low: Low-coverage data, CG* : Called genotypes from low-coverage data.

Next, we calculated the selection statistics along PC1 that display a north-south cline in the European populations. We find that both `PCAngsd-S1` and `PCAngsd-S2` statistics behaves as expected under the null hypothesis for most sites (Figure 4). Similarly the statistics obtained from `FastPCA` and `pcadapt` follows the expectation, although, the latter required genomic inflation correction [5], on both HQG and CG*. After multiple testing correction, all software identify two genomic regions with significant genetic differentiation overlapping two gene clusters: *LCT/MCM6* (chr2) and *OCA2/HERC2* (chr15) (Figure 4). These results are inline with previous research on these populations [1, 21, 27].

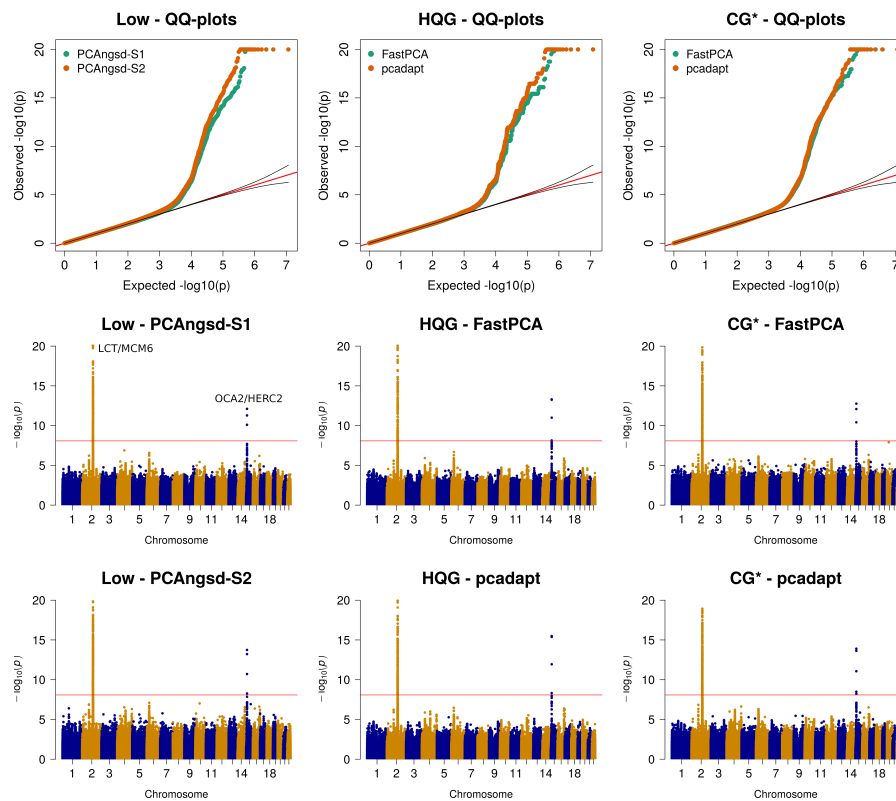


Figure 4: Selection scan of European populations. QQ and manhattan plots of the selection statistics from PCAngsd, FastPCA and pcadapt applied to the four European populations obtained. Red horizontal line is the Bonferroni adjusted significance level. PCAngsd-S2 and pcadapt has been corrected for genomic inflation. HQG: High quality genotype data, LOW: Low-coverage data, CG*: Called genotypes from low-coverage data.

For genotype calling from low-coverage data uncertain genotype calls are often excluded by applying a genotype quality threshold. After applying a genotype quality threshold of 20 both FastPCA and pcadapt identify within population biases on the first PC (see Figure 1 and 3). However, as the second PC to some extent recover the population structure, we applied FastPCA and pcadapt to the standard genotype calls. In the selection scan of the East Asian populations pcadapt recovered the same candidates regions as the HQG data, whereas FastPCA identified many false positive regions both on PC1 and PC2 (Figure S3). For the European populations, we observe highly inflated statistics on both PCs and many false positive selection signatures were identified genome-wide by both software (Figure S4). From these observations, it is evident that genotype calling of low-coverage data requires ad-hoc filters for each test scenario. Similarly, in a recent low coverage study Chiang and colleagues also used extensive filters, including machine learning algorithms, to exclude outlier samples and variants prior to computing the selection statistics for the Han chinese population [3]. In contrast, we show that the PCAngsd framework consistently obtain well-behaving selection statistics in both scenarios from low-coverage data without the need

for ad-hoc quality filters on either variant calls or sample selection.

A limitation of the PC-based selection scans are their capability of detecting selection in scenarios of non-continuous population structure. We show an example of this in Figure S5, where we have applied the three software to three populations with distinct ancestry (CEU, CHB, YRI). As also shown in the original study of **FastPCA** [7], it has low power in data sets with higher F_{ST} between the populations, where we see deflated test statistics due to being inversely scaled with the inferred large eigenvalues of the corresponding tested PC for **PCAngsd-S1** and **FastPCA**. We see the opposite pattern for **PCAngsd-S2** and **pcadapt**, where the test statistics are very inflated, even after correction with genomic control, leading to many false positives. We reckon that F_{ST} based selection scans are more appropriate in such scenarios with evident population clusters.

In conclusion, we have implemented two PC-based test statistics to perform selection scans in the **PCAngsd** (v.0.99) framework that performs iterative inference of population structure based on either GL or genotype data. This makes it possible to scan for selection genome-wide in data sets of low and/or variable coverage data sampled from genetically continuous populations. We show that the signatures of selection obtained from the low coverage in both the East Asian and European populations were on par with those from the high quality genotype data obtained from existing state-of-the-art software using called genotypes. The **PCAngsd** framework also reduces the need to rely on ad-hoc filters on SNP sites and/or samples. All obtained candidates for selection identified from the low-coverage data have been described in other studies targeting signatures of selection in European and East Asian ancestries. The **PCAngsd** framework is freely available at <https://github.com/rosemeis/pcangsd>.

5 Acknowledgements

The study was supported by the Lundbeck foundation.

References

- [1] Todd Bersaglieri, Pardis C Sabeti, Nick Patterson, Trisha Vanderploeg, Steve F Schaffner, Jared A Drake, Matthew Rhodes, David E Reich, and Joel N Hirschhorn. Genetic signatures of strong recent positive selection at the lactase gene. *American journal of human genetics*, 74(6):1111–1120, June 2004.
- [2] Jade Yu Cheng, Fernando Racimo, and Rasmus Nielsen. Ohana: detecting selection in multiple populations by modelling ancestral admixture components. February 2019.
- [3] Charleston W K Chiang, Serghei Mangul, Christopher Robles, and Sriram Sankararaman. A comprehensive map of genetic variation in the world’s largest ethnic Group-Han chinese. *Molecular biology and evolution*, 35(11):2736–2750, November 2018.
- [4] 1000 Genomes Project Consortium et al. A global reference for human genetic variation. *Nature*, 526(7571):68, 2015.
- [5] B Devlin and K Roeder. Genomic control for association studies. *Biometrics*, 55(4):997–1004, December 1999.

- [6] Shaohua Fan, Matthew E B Hansen, Yancy Lo, and Sarah A Tishkoff. Going global by adapting local: A review of recent human adaptation. *Science*, 354(6308):54–59, October 2016.
- [7] Kevin J Galinsky, Gaurav Bhatia, Po-Ru Loh, Stoyan Georgiev, Sayan Mukherjee, Nick J Patterson, and Alkes L Price. Fast principal-component analysis reveals convergent evolution of *adh1b* in europe and east asia. *The American Journal of Human Genetics*, 98(3):456–472, 2016.
- [8] Thorfinn Sand Korneliussen, Anders Albrechtsen, and Rasmus Nielsen. Angsd: analysis of next generation sequencing data. *BMC bioinformatics*, 15(1):356, 2014.
- [9] Panayiota Kotsakiozi, Joshua B Richardson, Verena Pichler, Guido Favia, Ademir J Martins, Sandra Urbanelli, Peter A Armbruster, and Adalgisa Caccone. Population genomics of the asian tiger mosquito, *aedes albopictus*: insights into the recent worldwide invasion. *Ecology and evolution*, 7(23):10143–10157, December 2017.
- [10] Richard B Lehoucq, Danny C Sorensen, and Chao Yang. *ARPACK users’ guide: solution of large-scale eigenvalue problems with implicitly restarted Arnoldi methods*. SIAM, 1998.
- [11] Heng Li. A statistical framework for SNP calling, mutation discovery, association mapping and population genetical parameter estimation from sequencing data. *Bioinformatics*, 27(21):2987–2993, November 2011.
- [12] Yong Fuga Li, James C Costello, Alisha K Holloway, and Matthew W Hahn. “reverse ecology” and the power of population genomics. *Evolution*, 62(12):2984–2994, December 2008.
- [13] Siyang Liu, Shujia Huang, Fang Chen, Lijian Zhao, Yuying Yuan, Stephen Starko Francis, Lin Fang, Zilong Li, Long Lin, Rong Liu, Yong Zhang, Huixin Xu, Shengkang Li, Yuwen Zhou, Robert W Davies, Qiang Liu, Robin G Walters, Kuang Lin, Jia Ju, Thorfinn Korneliussen, Melinda A Yang, Qiaomei Fu, Jun Wang, Lijun Zhou, Anders Krogh, Hongyun Zhang, Wei Wang, Zhengming Chen, Zhiming Cai, Ye Yin, Huanming Yang, Mao Mao, Jay Shendure, Jian Wang, Anders Albrechtsen, Xin Jin, Rasmus Nielsen, and Xun Xu. Genomic analyses from non-invasive prenatal testing reveal genetic associations, patterns of viral infections, and chinese population history. *Cell*, 175(2):347–359.e14, October 2018.
- [14] Keurcien Luu, Eric Bazin, and Michael G B Blum. pcadapt: an R package to perform genome scans for selection based on principal component analysis. *Mol. Ecol. Resour.*, 17(1):67–77, January 2017.
- [15] Prasanta Chandra Mahalanobis. On the generalized distance in statistics. 1936.
- [16] J Meisner and A Albrechtsen. Testing for Hardy-Weinberg equilibrium in structured populations using genotype or low-depth next generation sequencing data. *Molecular ecology resources*, 2019.
- [17] Jonas Meisner and Anders Albrechtsen. Inferring population structure and admixture proportions in low-depth ngs data. *Genetics*, 210(2):719–731, 2018.
- [18] Paolo Momigliano, Ann-Britt Florin, and Juha Merilä. Biases in demographic modelling affect our understanding of recent divergence. February 2021.

- [19] Kevin D Murray, Jasmine K Janes, Ashley Jones, Helen M Bothwell, Rose L Andrew, and Justin O Borevitz. Landscape drivers of genomic diversity and divergence in woodland eucalyptus. *Molecular ecology*, 28(24):5232–5247, December 2019.
- [20] Rasmus Nielsen, Thorfinn Korneliussen, Anders Albrechtsen, Yingrui Li, and Jun Wang. SNP calling, genotype calling, and sample allele frequency estimation from New-Generation sequencing data. *PloS one*, 7(7):e37558, July 2012.
- [21] Heather L Norton, Rick A Kittles, Esteban Parra, Paul McKeigue, Xianyun Mao, Keith Cheng, Victor A Canfield, Daniel G Bradley, Brian McEvoy, and Mark D Shriver. Genetic evidence for the convergent evolution of light skin in europeans and east asians. *Molecular biology and evolution*, 24(3):710–722, March 2007.
- [22] Caroline Pont, Thibault Leroy, Michael Seidel, Alessandro Tondelli, Wandrille Duchemin, David Armisen, Daniel Lang, Daniela Bustos-Korts, Nadia Goué, François Balfourier, Márta Molnár-Láng, Jacob Lage, Benjamin Kilian, Hakan Özkan, Darren Waite, Sarah Dyer, Thomas Letellier, Michael Alaux, Wheat and Barley Legacy for Breeding Improvement (WHEALBI) consortium, Joanne Russell, Beat Keller, Fred van Eeuwijk, Manuel Spannagl, Klaus F X Mayer, Robbie Waugh, Nils Stein, Luigi Cattivelli, Georg Haberer, Gilles Charmet, and Jérôme Salse. Tracing the ancestry of modern bread wheats. *Nature genetics*, 51(5):905–911, May 2019.
- [23] Florian Privé, Keurcien Luu, Bjarni J Vilhjálmsson, and Michael G B Blum. Performing highly efficient genome scans for local adaptation with R package pcadapt version 4. *Mol. Biol. Evol.*, 37(7):2153–2154, July 2020.
- [24] Vladimir Rokhlin, Arthur Szlam, and Mark Tygert. A randomized algorithm for principal component analysis. September 2008.
- [25] G Sallé, S R Doyle, J Cortet, J Cabaret, M Berriman, N Holroyd, and J A Cotton. The global diversity of haemonchus contortus is shaped by human intervention and climate. *Nature communications*, 10(1):4811, October 2019.
- [26] Marion Sinclair-Waters, Ian R Bradbury, Corey J Morris, Sigbjørn Lien, Matthew P Kent, and Paul Bentzen. Ancient chromosomal rearrangement associated with local adaptation of a postglacially colonized population of atlantic cod in the northwest atlantic. *Molecular ecology*, 27(2):339–351, January 2018.
- [27] Benjamin F Voight, Sridhar Kudaravalli, Xiaoquan Wen, and Jonathan K Pritchard. A map of recent positive selection in the human genome. *PLoS biology*, 4(3):e72, March 2006.
- [28] Hongru Wang, Filipe G Vieira, Jacob E Crawford, Chengcai Chu, and Rasmus Nielsen. Asian wild rice is a hybrid swarm with extensive gene flow and feralization from domesticated rice. *Genome research*, 27(6):1029–1038, June 2017.
- [29] Aryn P Wilder, Stephen R Palumbi, David O Conover, and Nina Overgaard Therkildsen. Footprints of local adaptation span hundreds of linked genes in the atlantic silverside genome. *Evolution letters*, 4(5):430–443, October 2020.
- [30] Xin Yi, Yu Liang, Emilia Huerta-Sanchez, Xin Jin, Zha Xi Ping Cuo, John E Pool, Xun Xu, Hui Jiang, Nicolas Vinckenbosch, Thorfinn Sand Korneliussen, Hancheng Zheng, Tao Liu,

Weiming He, Kui Li, Ruibang Luo, Xifang Nie, Honglong Wu, Meiru Zhao, Hongzhi Cao, Jing Zou, Ying Shan, Shuzheng Li, Qi Yang, Asan, Peixiang Ni, Geng Tian, Junming Xu, Xiao Liu, Tao Jiang, Renhua Wu, Guangyu Zhou, Meifang Tang, Junjie Qin, Tong Wang, Shuijian Feng, Guohong Li, Huasang, Jiangbai Luosang, Wei Wang, Fang Chen, Yading Wang, Xiaoguang Zheng, Zhuo Li, Zhuoma Bianba, Ge Yang, Xiping Wang, Shuhui Tang, Guoyi Gao, Yong Chen, Zhen Luo, Lamu Gusang, Zheng Cao, Qinghui Zhang, Weihang Ouyang, Xiaoli Ren, Huiqing Liang, Huisong Zheng, Yebo Huang, Jingxiang Li, Lars Bolund, Karsten Kristiansen, Yingrui Li, Yong Zhang, Xiuqing Zhang, Ruiqiang Li, Songgang Li, Huanming Yang, Rasmus Nielsen, Jun Wang, and Jian Wang. Sequencing of 50 human exomes reveals adaptation to high altitude. *Science*, 329(5987):75–78, July 2010.

Supplementary Material

Posterior expectation of the genotype

We are using the iterative algorithm in `PCAngsd` to estimate individual allele frequencies π [17]. With the assumption of Hardy-Weinberg proportions, we can derive the posterior genotype probability using the genotype likelihoods as follows for individual i in site j :

$$P(G_{ij} = g | X_{ij}, \hat{\pi}_{ij}) = \frac{P(X_{ij} | G_{ij} = g)P(G_{ij} = g | \hat{\pi}_{ij})}{\sum_{g'=0}^2 P(X_{ij} | G_{ij} = g')P(G_{ij} = g' | \hat{\pi}_{ij})}, \quad (\text{S1})$$

$$P(G_{ij} = g | \hat{\pi}_{ij}) = \begin{cases} \hat{\pi}_{ij}^2, & g = 0, \\ 2\hat{\pi}_{ij}(1 - \hat{\pi}_{ij}), & g = 1, \\ (1 - \hat{\pi}_{ij})^2, & g = 2. \end{cases}$$

Here g is the genotype and $P(X | G = g)$ is the genotype likelihood. The posterior expectation of the genotype is thus given by:

$$\mathbb{E}[G_{ij} | X_{ij}, \hat{\pi}_{ij}] = \sum_{g=0}^2 g P(G_{ij} = g | X_{ij}, \hat{\pi}_{ij}), \quad (\text{S2})$$

which we use in our selection statistics to account for uncertainty in the genotypes in low-coverage data.

Supplementary figures

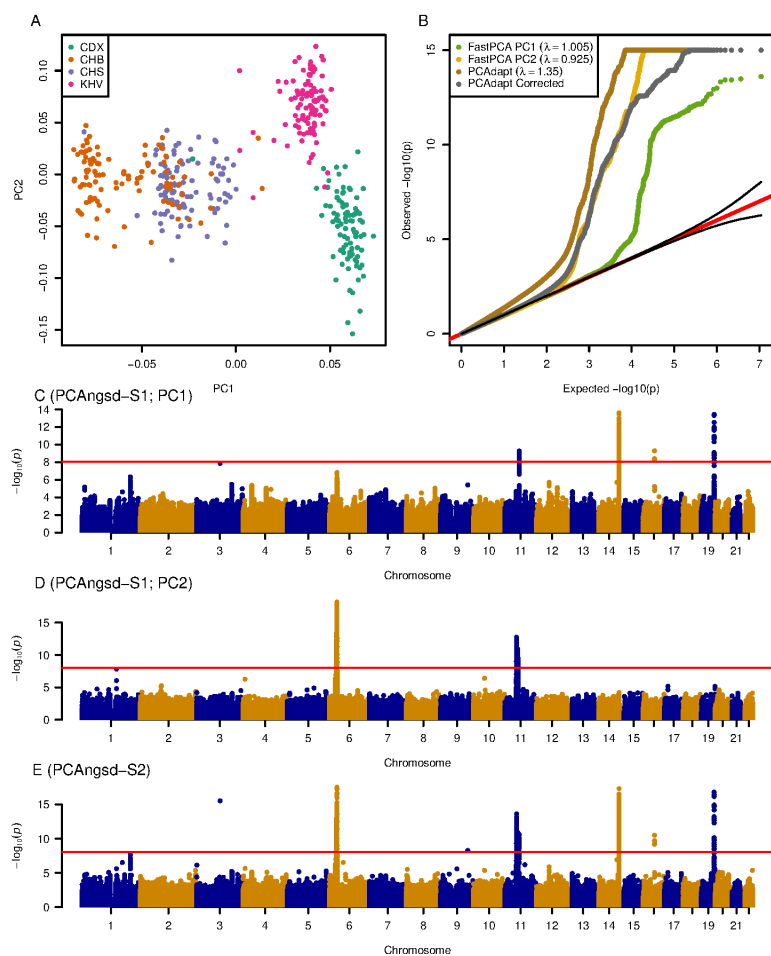


Figure S1: PCAngsd results on the high quality genotype dataset of the Asian populations in the 1000 Genomes Project. PCA plot of the four Asian populations showing the separation of Northern and Southern Asia on PC1 and PC2 separating KHV and CDX (A). QQ-plot of the test statistics, including PCAngsd-S2 statistics before and after genomic inflation correction (B). Manhattan plot of the selection scan of PC1 (C) and PC2 (D) based on the PCAngsd-S1 statistic and PCAngsd-S2 (E) of both PCs. Manhattan plots from PCAngsd-S2 has been corrected for genomic inflation. Red horizontal line is the Bonferroni adjusted significance level.

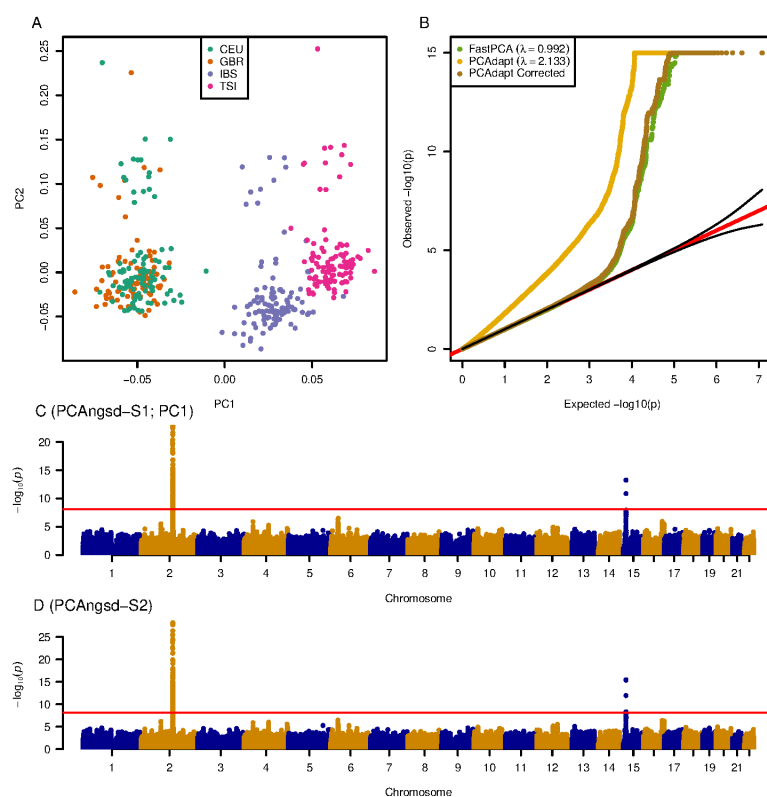


Figure S2: PCAngsd results on the high quality genotype dataset of the European populations in the 1000 Genomes Project. PCA plot of the four European populations showing the separation of Northern and Southern Europe on PC1 (A). QQ-plot of the test statistics, including PCAngsd-S2 statistics before and after genomic inflation correction B. Manhattan plot of the selection scan based on the PCAngsd-S1 (C) and PCAngsd-S2 (D) test statistics along PC1. Manhattan plots from PCAngsd-S2 has been corrected for genomic inflation. Red horizontal line is the Bonferroni adjusted significance level.

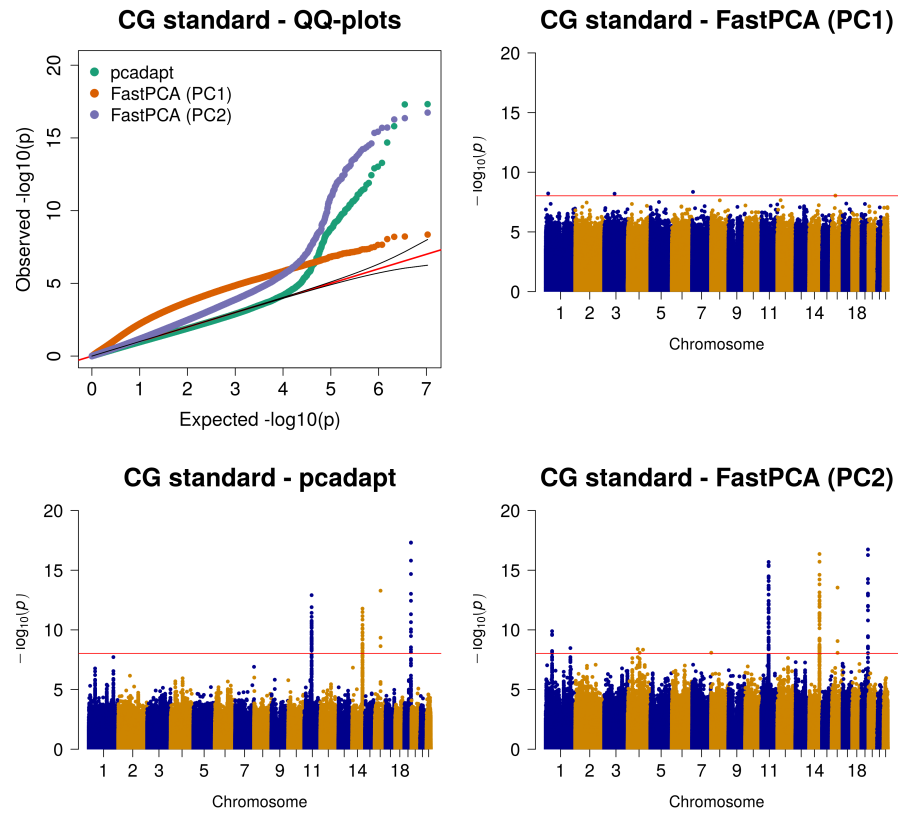


Figure S3: PC1 against PC2, QQ-plots and Manhattan plots of the selection statistics from FastPCA and pcadapt applied to the four East Asian populations obtained. Red horizontal line is the Bonferroni adjusted significance level. pcadapt has been corrected for genomic inflation. CG standard: Called genotypes from low-coverage data with a genotype quality threshold on 20.

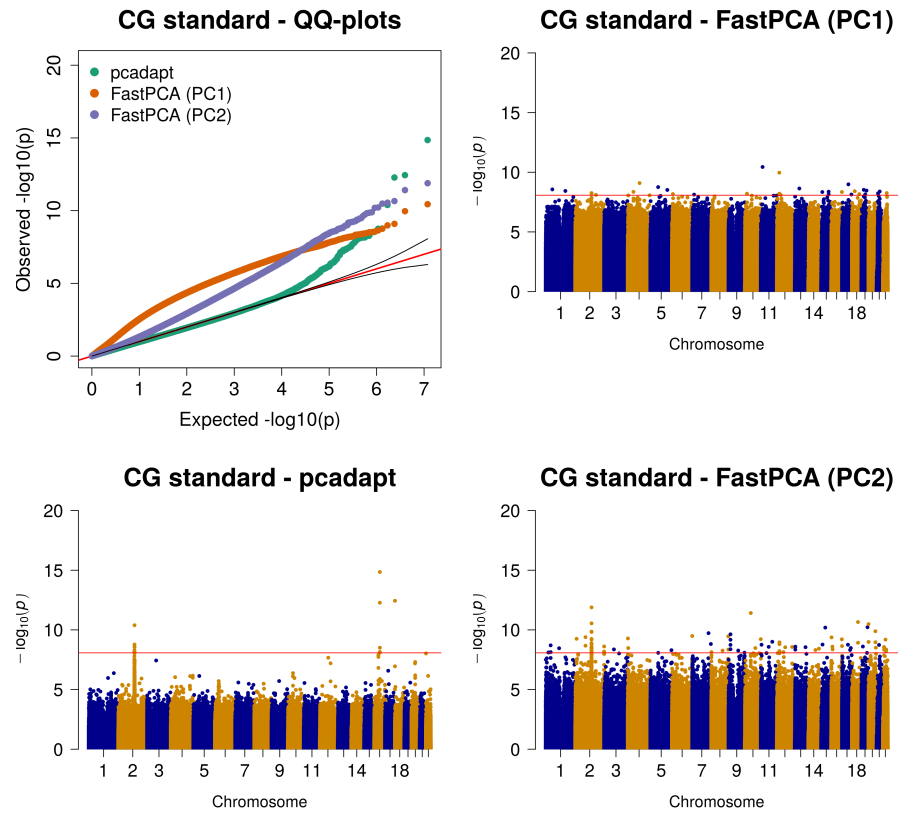


Figure S4: PC1 against PC2, QQ-plots and Manhattan plots of the selection statistics from FastPCA and pcadapt applied to the four European populations obtained. Red horizontal line is the Bonferroni adjusted significance level. pcadapt has been corrected for genomic inflation. CG standard: Called genotypes from low-coverage data with a genotype quality threshold on 20.

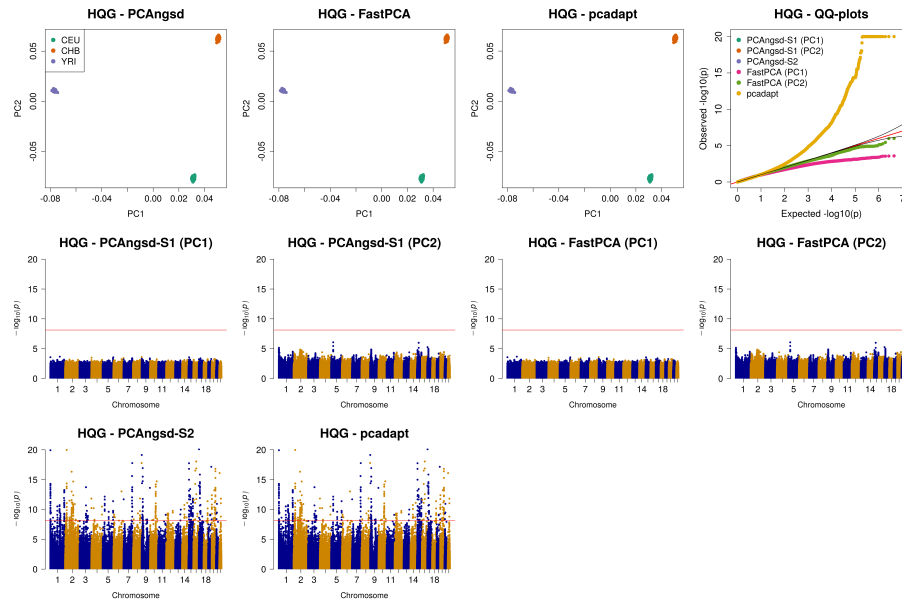


Figure S5: PC1 against PC2, QQ-plots and Manhattan plots of the selection statistics obtained from PCAngsd, FastPCA and pcadapt applied to a European (CEU), Asian (CHB), and African (AFR) population. Red horizontal line is the Bonferroni adjusted significance level. pcadapt has been corrected for genomic inflation. HQG: High quality genotype data.

Chrom	ID	Position	A1	A2	F	<i>p</i> -value
3	rs149768401	100365528	C	G	-0.40	1.20×10^{-12}
6	rs41542812	32629931	G	C	0.086	0.42
9	rs115349067	117013044	C	A	-0.26	1.26×10^{-7}
11	rs7101761	49598178	G	A	-0.068	0.071
11	rs72643559	61620274	C	T	-0.039	0.23
14	rs1071803	106209119	T	C	0.022	1
16	rs17822931	48258198	C	T	-0.015	0.64
19	rs434124	54809336	C	G	-0.011	1

Table S1: Hardy-Weinberg equilibrium test using PCANGSD on the HQG data from the four East Asian populations. The table only contains the significant top hits from the selection analyses. F: inbreeding coefficient.